Food Chemistry: X 24 (2024) 102012

Contents lists available at ScienceDirect

Food Chemistry: X

journal homepage: www.sciencedirect.com/journal/food-chemistry-x

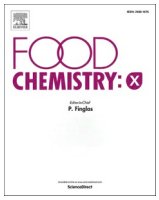

Characterization and application of Cinnamaldehyde-loaded zein nanoparticles in a polyvinyl alcohol/chitosan film for silver pomfret (*Pampus argenteus*) packaging

Zhan Zhang [a,b], Xiaojun Zhang [b,a,*], Bing Lin [a,b], Yaqian Zhong [a,b], Wenxiu Zhang [a,b], Shangrong Zhong [a,b], Xiaxia Chen [b,a]

[a] College of Food and Pharmacy, Zhejiang Ocean University, Zhoushan, 316022, China
[b] Zhejiang Marine Fisheries Research Institute, Zhoushan, 316021, China

ARTICLE INFO

Keywords:
Zein
Cinnamaldehyde
Nanoparticles
Active packaging films
Preservation

ABSTRACT

This study aims to prepare and characterize cinnamaldehyde-loaded zein/sodium alginate nanoparticles (ZCNPs) and incorporate them into polyvinyl alcohol/chitosan (PVA/CS) bioactive films (PSCN) to investigate their compatibility, physicochemical properties, and their application as a preservation material for pomfret fish. The results indicate that the anionic sodium alginate coating improved the particle size, zeta potential, and PDI of zein nanoparticles. The ZCNPs were uniformly dispersed within the films, enhancing the mechanical properties and water vapor barrier performance. The X-ray diffraction (XRD) and Fourier transform infrared (FTIR) analyses confirmed the amorphous structure of the films and the formation of hydrogen bonds. In the PVA/CS film, with the increase of ZCNPs, the thermal decomposition temperature of the film increased from 298 °C to 308 °C, while the film thickness and water contact angle were not significantly affected, remaining around 0.31 cm and 23°, respectively. Additionally, after the incorporation of ZCNPs, the DPPH radical scavenging rate of the film increased from 14.58 % to 95.38 %, significantly delaying the quality deterioration of pomfret during storage.

1. Introduction

In recent years, As consumer demand for fresh food increases, food preservation technology has become a key focus of research in the field of food science (Zhang et al., 2023). Therefore, the development of biodegradable active packaging has garnered significant attention to address microplastic pollution caused by non-degradable petroleum-based plastic packaging (Ludwicka, Kaczmarek, & Białkowska, 2020). Moreover, the unique antibacterial, antioxidant, and light-blocking properties of natural polymer packaging can extend the shelf life of food, making biodegradable natural polymer food packaging research imperative in the field of food packaging (Panda, Sadeghi, & Seo, 2022). In the current literature, lipids, proteins, and polysaccharides have emerged as the primary materials for biodegradable natural biopolymer packaging due to their biodegradability, film-forming properties, and cost-effectiveness (Hosseini & Gómez-Guillén, 2018).

Chitosan is a cationic polysaccharide obtained through the deacetylation of chitin extracted from shrimp and crab shells under alkaline conditions (Hua et al., 2021). It is composed of D-glucosamine and *N*-acetyl-d-glucosamine units (Chen et al., 2023). Because of its antioxidant properties, non-toxicity, and biocompatibility, chitosan has become one of the most widely used active food packaging materials. Research indicates that chitosan-metal oxide films and chitosan-modified graphene (oxide) films significantly inhibit the growth rates of *Campylobacter jejuni* and *Listeria monocytogenes* (Wrońska et al., 2021). However, chitosan films have drawbacks such as poor mechanical performance and water resistance, limiting their use as food packaging materials (Wang, Li, Wu, Li, & Li, 2024). Mixing chitosan with other natural polymers has been reported to be an effective strategy to improve its properties (Tan et al., 2024).

PVA is an excellent semi-crystalline polymer for film formation, characterized by strong biocompatibility and mechanical properties. The United States Department of Agriculture (USDA) has approved PVA films for packaging meat products (Haghighi et al., 2020). Liu et al. (2023) demonstrated that PVA/CS films obtained by blending PVA and CS using the solution mixing method greatly increase tensile strength due to the formation of intermolecular hydrogen bonds between PVA and CS. Furthermore, CS imparts antimicrobial properties to the films.

* Corresponding author at: Zhejiang Marine Fisheries Research Institute, Zhoushan 316021, China.
E-mail address: zhangxj@zjou.edu.cn (X. Zhang).

https://doi.org/10.1016/j.fochx.2024.102012
Received 24 July 2024; Received in revised form 29 October 2024; Accepted 13 November 2024
Available online 15 November 2024

Despite the improved performance over pure CS, the reduced stability in humid environments and weaker antimicrobial properties of PVA/CS prevent it from meeting the shelf-life requirements for meat products, significantly limiting its practical utility (Yu, Li, Chu, & Zhang, 2017).

Currently, substances such as cinnamon, anthocyanins, epigallocatechin gallate, and brassinolide exhibit antioxidant, antibacterial, and biohormonal effects, playing a significant role in the field of food preservation (Ban et al., 2024; Guo et al., 2024; Yang et al., 2021). Cinnamon essential oil is extracted from the bark of cinnamon trees, with cinnamon aldehyde being its primary component (H. Chen et al., 2016). Cinnamaldehyde is a natural antimicrobial compound that inhibits bacterial growth by suppressing ATPase activity, cell wall biosynthesis, and cell membrane integrity (Shreaz et al., 2016). The US Food and Drug Administration recognizes cinnamaldehyde as a safe natural active ingredient for use in food (Doyle & Stephens, 2019). However, cinnamaldehyde is unstable to light and heat, and its rapid release rate within biopolymers makes it challenging to use efficiently. Loading natural active ingredients onto nanoparticles is currently the most effective way to improve their stability. Zein is a food-grade protein that is amphiphilic, biocompatible, and self-assembling, is widely used in current research to fabricate nanoparticles for encapsulating active ingredients (Yavari Maroufi, Ghorbani, Tabibiazar, Mohammdi, & Pezeshki, 2021). Sodium alginate is a linear anionic polysaccharide with an opposite charge to zein nanoparticles. Its ability to encapsulate hydrophobic substances helps to improve the stability of zein nanoparticles and efficiently address aggregation concerns during storage (Lim et al., 2020).

Silver pomfret *(Pampus argenteus)* is mainly distributed in the Bohai Sea and East China Sea in China. It is known for its delicate flesh and rich content of long-chain n-3 polyunsaturated fatty acids and protein, which has led to an enormous market demand (Wu et al., 2016; Zhao, Zhuang, Song, Shi, & Zhang, 2010). However, silver pomfret is a highly perishable food, making it susceptible to quality deterioration due to lipid oxidation, microbial contamination, and protein degradation, resulting in a reduced shelf life (Zhao et al., 2021). Therefore, applying PVA/CS films that contain loaded ZCNPs to silver pomfret is an effective method for extending its freshness and shelf life.

In this study, we aimed to prepare PVA/CS active packaging films loaded with ZCNPs, and evaluate the encapsulation effect of SA on the nanoparticles as well as the controlled release effect of cinnamaldehyde. The barrier properties, mechanical properties, thermal stability, and antibacterial and antioxidant properties of the films were investigated. Finally, the films were applied to silver pomfret to assess their potential as active food packaging. In summary, this study establishes a theoretical basis for the development of biodegradable bioactive films.

2. Materials and methods

2.1. Materials

Pomfret was purchased from China Aquatic Products Zhoushan Marine Fishery Company. Chitosan, glacial acetic acid, anhydrous calcium chloride were purchased from Sinopharm Chemical Reagent Co., Ltd. (Shanghai, China). Corn gluten and cinnamaldehyde were purchased from Yien Chemical Technology Co., Ltd. (Shanghai, China). Polyvinyl alcohol was purchased from Aladdin Biochemical Technology Co., Ltd. (Shanghai, China). The DPPH kit was bought from the Institute of Bioengineering, Nanjing, China. All the chemical reagents were analytically pure.

2.2. Methods

2.2.1. Preparation of nanoparticle systems

The nanoparticles were prepared using anti-solvent co-precipitation (ASCP) based on the method of Liu, Jing, Han, Zhang, and Tian (2019) with some modifications. Cinnamaldehyde (CIN) was dissolved at a concentration of 3 % (*w/v*) with zein (20 mg/mL) in 75 % ethanol. Then, 10 mL of this solution was gradually added to 40 mL of sodium alginate (1, 2, 5, 10, and 20 mg/mL) and adjusted to pH 3.5, while stirring for 30 min. The ethanol was evaporated using a rotary evaporator (R-215, Büchi AG, Switzerland), and the nanoparticle dispersion was centrifuged at 3000 ×*g* for 10 min to discard large particles and unencapsulated cinnamaldehyde. The dispersion was refilled to 50 mL with water at pH 3.5. The pH was adjusted to 3.5 using 1 M HCl to obtain the CIN-loaded zein-SA nanoparticle dispersion. Finally, the nanoparticle dispersion was vacuum freeze-dried (K-350, Büchi AG, Switzerland) to obtain nanoparticles and stored at −18 °C for future use. The nanoparticles were named as zein-SC1, zein-SC2, zein-SC5, zein-SC10, and zein-SC20 based on the concentration of the SC solution.

2.3. Characterization of nanoparticles

2.3.1. Particle size and zeta potential of nanoparticles

The particle size and zeta potential of the nanoparticles were measured following the method of Chen et al. (2021), with minor modifications. The nanoparticles were diluted tenfold in deionized water at pH 3.5 and characterized for particle size, zeta potential, and polymer dispersity index (PDI) at room temperature using a Zetasizer NanoZS90 (Malvern Instruments Ltd., UK). Each sample was measured three times, and the results were averaged.

2.3.2. Determination of encapsulation efficiency and loading capacity of nanoparticles

The content of free cinnamaldehyde was determined using an organic solvent extraction method. 15 mg of nanoparticle powder was dispersed in 20 mL of n-hexane, vortexed for 5 s, and the supernatant was extracted. The absorbance was measured at 285 nm using a UV spectrophotometer. The total cinnamaldehyde content was determined using an organic solvent extraction method. 15 mg of nanoparticle powder was dispersed in 1 mL of ethanol at 40 °C, stirred for 5 min, ultrasonicated for 20 min, then centrifuged at 4000 r/min for 5 min. The ethanol was washed and centrifuged three times; all the supernatants obtained were combined and the ethanol was evaporated at 40 °C using a rotary evaporator until the total volume reached 1 mL. The absorbance was measured at 285 nm. Based on the free cinnamaldehyde and total cinnamaldehyde content in the nanoparticles, the encapsulation efficiency and loading capacity were calculated. The calculation formulas are as follows (Mondéjar-López et al., 2023):

$$EE\% = \frac{encapsulated\ CIN}{CIN\ input} \times 100\% \quad (1)$$

$$LC\% = \frac{encapsulated\ CIN}{total\ amount\ of\ CIN\ zein\ SA} \times 100\% \quad (2)$$

2.3.3. Scanning Electron microscopy (SEM)

The powder obtained from vacuum freeze-drying of cinnamaldehyde-zein nanoparticles was imaged using a scanning electron microscope (FWI QUANTA FEG650, ZEISS, Germany) at an accelerating voltage of 3.0 kV, and a gold sputter coating was applied to the sample before imaging.

2.4. Preparation of the film

The films were prepared following the procedure described by Hosseini, Ghaderi, and Gómez-Guillén (2021) with slight modifications. Initially, polyvinyl alcohol (PVA) solution (4 % *w/v*) and chitosan solution (1 % w/v) were prepared in deionized water and acetic acid solution (2.0 wt%) at 90 °C and 50 °C, respectively. The PVA solution was cooled to room temperature before being uniformly mixed with nanoparticle dispersion (5 %, 10 %, 15 % *v*/v). The chitosan solution was then added to achieve a PVA/chitosan solution weight ratio of 1:1.

Glycerol (1 % v/v) was added to the PVA/chitosan solution. The control group consisted of thin films without the addition of nanoparticles. The film-forming solution was poured onto 90 mm petri dishes and dried at 40 °C. The films were then peeled off and equilibrated in a desiccator for 48 h. The films were named PCSN0, PCSN5, PCSN10, and PCSN15 based on the concentration of nanoparticle dispersion.

2.5. Structure and morphology of the film

2.5.1. Scanning Electron microscopy (SEM)

The film cross-sections were cryo-fractured using liquid nitrogen and mounted onto a specialized cross-section sample holder. The surface and cross-sectional microstructures of the films were characterized using a scanning electron microscope (SEM) at an accelerating voltage of 15 kV, after which gold sputter coating was applied to the samples prior to imaging.

2.5.2. Fourier transform infrared spectroscopy(FTIR)

The film samples were mounted on a Fourier Transform Infrared (FTIR) spectrometer (PerkinElmer, Spectroscopy version 10.03.06, Waltham, MA, USA) equipped with Attenuated Total Reflection (ATR). The infrared spectra of the films were acquired by scanning 32 times at a spectral resolution of 4000–650 cm^{-1}, with a 4 cm^{-1} interval. The functional groups of the film samples were analyzed by identifying the positions of the absorption peaks in the spectra (Huang, Ge, Zhou, & Wang, 2022).

2.5.3. X-ray diffraction (XRD)

The diffraction patterns of the films were recorded using an X-ray diffractometer (D5000, Siemens, Germany) at 40 kV and 40 mA, using a copper target (Kα, λ = 1.5406 Å) (Zou, Sun, Shi, Wan, & Zhang, 2022). The data were collected over a 2θ range of 5°-90°, with a step size of 5°/min.

2.5.4. Thermogravimetric analysis (TGA)

All film samples weighing 4–5 mg were placed in a dry environment, and their thermal stability and decomposition temperature were determined using a thermogravimetric analyzer (TG 209 F3 Tarsus, NETZSCH, Germany) at a nitrogen flow rate of 20 mL/min. The temperature was escalated from room temperature to 700 °C at a heating rate of 25 °C/min. The results were recorded as DTG and TG scan curves.

2.5.5. Mechanical properties of the film

The thickness of the nanocomposite films was measured at six different locations using a micrometer (JC14241, Yousu, China), and the average value was used as the measurement. The mechanical properties of the films, including tensile strength (TS) and elongation at break (EB), were measured at room temperature using an Electronic Universal Testing Machine (INSTRON 5982; Instron, US). Each film sample (400 mm × 100 mm) was positioned between two clamps, with an initial distance of 60 mm between them. The sample was stretched at a rate of 50 mm/min until it broke. The calculations for TS and EB are as follows:

$$TS(MPa) = \frac{F_m}{w \times d} \tag{3}$$

where *TS* is the tensile strength of the film (MPa); F_m is the maximum force (N) that the film withstands at the point of rupture; *w* is the width of the film sample (mm); *d* is the thickness of the sample (mm).

$$EB(\%) = \frac{L_1 - L_0}{L_0} \times 100 \tag{4}$$

where *EB* is the elongation at break of the film (%); L_1 is the maximum elongation length (mm) the film reaches at the point of rupture; L_0 is the initial gauge length (mm).

2.5.6. Water resistance of the film

The moisture content (MC), swelling index (SI), and water solubility (WS) of the films were determined according to the methods reported in the literature, with some modifications (Al-Maqtari et al., 2022). The film samples (2 cm × 2 cm) were weighed after reaching equilibrium humidity. The samples were then dried in an oven at 105 ± 1 °C to attain a constant weight (M_1), which was recorded. The moisture content of the samples was calculated as a percentage of the weight loss. To assess water solubility, dried samples (M_1) were immersed in distilled water and continuously stirred at 25 °C for 24 h. The initial weight of the film was M_1, its weight after soaking was M_2 and then the film was dried in an oven at 105 ± 1 °C, and the weight was recorded as M_3 to determine the water retention of the film. The moisture content (MC), swelling index (SI), and water retention (WS) of the film were calculated using the following formulas:

$$MC(\%) = (M_0 - M_1)/M_0 \times 100 \tag{5}$$

$$SI(\%) = (M_2 - M_1)/M_1 \times 100\% \tag{6}$$

$$WS(\%) = (M_2 - M_3)/M_2 \times 100 \tag{7}$$

Water vapor permeability (WVP) measurements were conducted according to ASTM E96–95 standard, with slight modifications. Each set of film samples was sealed with wax and placed in test tubes with anhydrous calcium chloride as a desiccant. The samples were then placed in a humidity chamber with a constant temperature, and the weight of the test tubes was intermittently monitored every hour until a constant weight (mass less than 0.001 g) was achieved. The weight was recorded as M_2. The WVP of the film was determined by the following formula:

$$WVP = \frac{(W_2 - W_1)\chi}{A \times t \times \Delta P} \tag{8}$$

where (W_2-W_1) is the mass of water in the film (g), χ is the thickness of the film (m), A is the permeation area of the film (m^2), t is time (s), and ΔP is the pressure difference across the film (Pa).

The water contact angle (WCA) of the samples was measured using a PG-X goniometer with the sessile drop method. 5 μL of deionized water was gently dropped onto the surface of the film using a micro syringe, and the contact angle between the film surface and the water droplet was measured and photographed within 10 s.

2.5.7. Antioxidant analysis of the film

Antioxidant activity was evaluated using the DPPH free radical scavenging method. Mix the film sample with 3 mL of methanol solution, centrifuged at 4000 rpm for 5 min, and the supernatant was mixed with 5 mL of DPPH solution (0.1 mmol/L). The mixture was allowed to stand in the dark for 30 min, and the absorbance of the solution was measured at 517 nm and 734 nm using a UV–visible spectrophotometer. The percentage of DPPH scavenging was calculated using the following formula (Li et al., 2023):

$$DPPH\ radical\ scavenging\ activity(\%) = \frac{(A_0 - A_1)}{A_0} \times 100 \tag{9}$$

where A0 represents the absorbance of the blank solution, and A1 represents the absorbance of the nanocomposite dispersion.

2.6. The preservation effect of PCSN film on silver pomfret

2.6.1. Preparation of aquatic product samples

The ice-fresh silver pomfret, purchased from Zhoushan Marine Fishery Company, was placed in ice slurry and promptly transferred to the laboratory, with the head and tail removed and only the middle portion retained. Based on the four types of films prepared in Section 2.4, namely PCSN0, PCSN5, PCSN10, and PCSN15, we used them to

wrap silver pomfret (3 cm × 5 cm), with regular plastic wrap used as the control group for comparison in preservation. The five groups of silver pomfret were placed in sterilized boxes and stored in a refrigerator at 4 °C for 12 days, with samples collected every 48 h. Subsequently, they were stored in the same sterile boxes in the refrigerator at 4 °C.

2.6.2. pH

5 g of crushed silver pomfret samples were weighed and 37.5 mL of distilled water was added, shook well, and the resulting mixture was filtered using a double-layer filter paper after 30 min to obtain the filtrate. The pH value of the filtrate for each group of samples was then measured (Lin, Zhang, Huang, & Li, 2023).

2.6.3. Thiobarbituric acid reactive substances

5 g of crushed silver pomfret samples were accurately weighed and mixed with 50 mL of 7.5 % trichloroacetic acid (TCA). Further, the mixture was allowed to stand for one hour in a water bath with gentle heating and agitation. The homogenate mixture was then filtered using double-layer filter paper to remove fats. After filtration, 5 mL of the supernatant was mixed with 0.02 mol/L Thiobarbituric acid (TBA) solution, placed in a water bath at 90 °C until it turned pink, and then quickly transferred to an ice bath. The absorbance of the solution was measured at 532 nm and 600 nm. The results are expressed as milligrams of malondialdehyde (MDA) equivalents per kilogram of sample (mg MDA/kg) (Wang, Chen, & Xie, 2022).

$$\text{Thiobarbituric Acid Reactive Substances}\left(\text{mg}\frac{\text{MDA}}{\text{kg}}\right) = \frac{(A532nm - A600nm)}{155 \times 0.1 \times 72.06} \times 100 \quad (10)$$

where A532 nm is the absorbance value at 532 nm, A600 nm is the absorbance value at 600 nm, 155 is the molar absorption coefficient of malondialdehyde (MDA) (the absorbance of 1 mmol of MDA in 1 L solution), and 72.06 is the molecular weight of MDA.

2.6.4. TVB-N

The sample was minced, mixed with distilled water, and filtered to obtain the supernatant. The mixture was subsequently analyzed using an automatic Kjeldahl nitrogen analyzer (Kjeltec 8400, FOSS, Denmark). The TVB-N results are expressed as mg of TVB-N per 100 g of sample.

2.6.5. TVC

Briefly, 25 g of silver pomfret sample was weighed and homogenized with 225 mL of phosphate buffer. 1 mL of the sample was added to 9 mL of diluent to prepare a 10-fold diluted sample solution. Then, 1 mL of the sample solution was added to a petri dish and 12–15 mL of agar was poured to create a plate count agar medium and then incubated aerobically at 30 °C for 72 h. The dilution factor and colony count were recorded. The colony count is expressed in colony-forming units (log CFU/g) (Zhang et al., 2023).

2.7. Statistical analysis

All experiments were performed in triplicate, and the data are presented as mean ± standard deviation. Data was analyzed using one-way analysis of variance (ANOVA) in SPSS Statistics 27.0, followed by Duncan's multiple range test ($P < 0.05$). Figures and charts were prepared using Origin Pro 2021.

3. Results and discussion

3.1. Structural characteristics of nanoparticles

3.1.1. Particle size and zeta potential of nanoparticles

The zeta potential, particle size, and PDI of Zein-SC nanoparticles with different mass ratios are shown in Fig. 1A and B. Previous research has shown that zein nanoparticles without added biopolymers or surfactants exhibit a positive charge at pH 3.5 (Roy et al., 2022). The zeta potentials of nanoparticles with different amounts of SC addition were −34.2, −8.8, −10.2, −35.3 and −31.5 mV, respectively. Zein-SC exhibited a negative charge with the addition of SA, reaching a minimum of −35.3 mV at 10 mg/mL. This is most likely owing to the negative charge of sodium alginate, which adsorbs onto the surface of zein, and causes a reduction in zeta potential (Yao, Chen, Song, McClements, & Hu, 2017).

We observed that the particle size of the nanoparticles decreases initially and then increases with the addition of SA. The particle size range of nanoparticles with different amounts of SC addition ranged from 197 nm to 425 nm. This may be due to bridging flocculation caused by the low SA content in zein-SC1. As the SA content increases, the particle size decreases, indicating that an adequate amount of SA can entirely encapsulate zein, resulting in particles of stable sizes (Hu & McClements, 2015). However, when the SA concentration exceeds a certain level, the particle size increases instead. This might be owing to excess SA adsorbing onto the zein surface, increasing the particle size of zein-SC and leading to aggregation. The PDI is a parameter used to determine the distribution uniformity of lipid nanoparticle systems, typically ranging from 0 to 1. The results showed that the PDI of nanoparticles with different amounts of SC addition ranged from 0.199 to 0.277. A PDI stabilized below 0.3 indicates that the particle size distribution of zein-SC is relatively uniform. The findings demonstrate that SA can improve the stability of zein nanoparticles. The addition of 5 mg of sodium alginate was the optimal amount to coat zein nanoparticles and further studies were conducted using this mass ratio.

3.1.2. Encapsulation efficiency and loading rate of nanoparticles

Encapsulation efficiency (EE) and loading capacity (LC) are indicators used to evaluate the effectiveness and performance of active ingredient encapsulation in nanoparticle carriers. Fig. 1 C and D shows the EE and LC of zein nanoparticles mixed with sodium alginate for cinnamaldehyde. EE ranges from 18.3 %–24.6 % and LC ranges from 53.5 %–77.5 %. With the addition of sodium alginate, both the EE and LC rose, reaching 24.6 % and 77.5 % for zein-SC2 respectively. This may be because the addition of sodium alginate promotes the formation of spatial hindrance within the nanoparticles, restricting the movement of cinnamaldehyde within the nanoparticles and reducing its release, resulting in controlled release (Ye et al., 2023). The EE and LC of zein-SC5, zein-SC10, and zein-SC20 decreased, indicating that the nanoparticles do not show linear increases in the encapsulation efficiency and loading capacity of the active ingredient with increasing sodium alginate. Liu et al. (2022) encapsulated apigenin (API) in zein-based nanoparticles and stabilized them using whey protein and carboxymethyl cellulose (CMC). Similarly, they found that the EE and LC of ZWC initially of ZWC initially increased and then decreased. The addition of lipids or polysaccharides affects the encapsulation efficiency and loading capacity of nanoparticles. Addition of an appropriate amount of sodium alginate can enhance the stability of cinnamaldehyde.

3.1.3. SEM morphological analysis

The morphology of zein-SC was studied by SEM, as shown in Fig. 2. Studies indicate that pure zein nanoparticles exhibit a compact and smooth spherical structure (Davidov-Pardo, Joye, & McClements, 2015). Fig. 2A shows zein nanoparticles with 1 mg of SA not only display spherical particles, but also aggregation of the nanoparticles. This may be because SA adsorbs onto the nanoparticle surface via electrostatic interactions and hydrogen bonding during the freeze-drying process (Fan, Yan, Xu, & Ni, 2012). Fig. 2 (B to E) illustrate electron microscopy images of nanoparticles following an increase in SA concentration. As the SA concentration increases, a single alginate molecule adsorbs on the surface of multiple zein nanoparticles, making them clusters, resulting in rough and irregular film-like surfaces. This may be attributed to

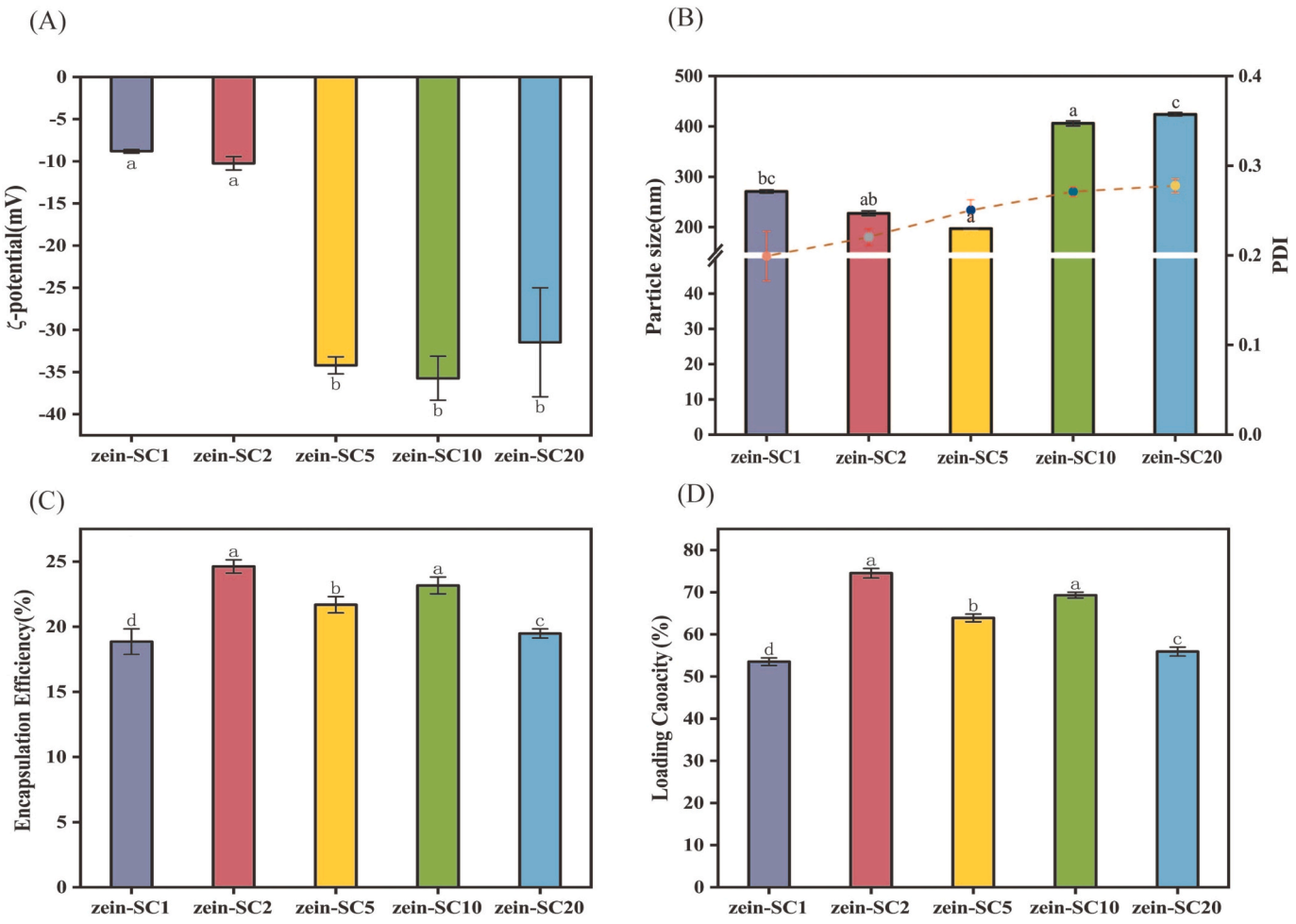

Fig. 1. Effects of SC to zein mass ratio on the (A) zeta-potentials, (B) particle sizes and PDI, (C) EE, (D) LC of the zein-sc.

excessive SA adsorption on the surface of nanoparticles, which forms a coating that results in the rough and complex network structure on the surface. Furthermore, studies have demonstrated that freeze-drying prior to SEM observation can significantly increase the roughening of nanoparticle surfaces. Chang, Wang, Hu, and Luo (2017) prepared a system of zein/caseinate/pectin nanoparticles using solvent precipitation. They observed irregular or film-like structures during the freeze-drying process of the nanoparticles. Upon rehydration, the nanoparticles reverted to their uniform spherical shape. These findings demonstrate that SA successfully coated on the nanoparticles, increasing their stability. We selected zein-SC5, which performed the best, for the subsequent studies.

3.2. Characterization analysis of PCSN films

3.2.1. SEM

The surface and cross-sectional structure of food packaging films determine their barrier properties and mechanical performance, directly influencing their functionality in packaging. To ascertain if the nanoparticles were successfully incorporated into the film, SEM analysis was performed to examine the surface and cross-sectional structures of the films. The surface of the PVA/CS film exhibited fine textures and small pores, while the cross-section displayed wavy wrinkles as shown in Fig. 3A and a, indicating poor compatibility between PVA and CS (Narasgoudr, Hegde, Vanjeri, Chougale, & Masti, 2020). As shown in Fig. 3 (B to D and b to d), the addition of nanoparticles alters the microstructure of the PVA/CS-based films. The film surface becomes rougher, with small particle protrusions and wrinkles. This is likely due to the formation of small aggregates of proteins and polysaccharides during the hot air-drying process, which leads to surface unevenness. Additionally, the PCSN15 surface exhibits a more pronounced convex structure, which is due to the uneven distribution of high-concentration nanoparticles in the film matrix. The cross-sectional analysis revealed that the nanoparticle-containing film was denser and rougher, which was most likely owing to strong bonding interactions between the nanoparticles and the film polymers. Wang et al. (2019) reported similar results when tea polyphenol-loaded chitosan nanoparticles were mixed with gelatin film. Overall, the cross-section and surface of the film with added nanoparticles did not show cracks or pores, suggesting good compatibility between the nanoparticles and the film matrix, significantly improving the film's performance, and fulfilling the requirements for active food packaging.

3.2.2. FTIR

The bonding interactions between films containing different amounts of ZCNPs and the ZCNPs themselves were identified using Fourier Transform Infrared (FTIR) spectroscopy. Fig. 4A shows the FTIR spectra of the four groups of nanocomposite films. The region between 3600 cm^{-1} and 3100 cm^{-1} corresponds to the amide A region, which generates peaks owing to the stretching vibration of the O—H group. Peaks at 1647 cm^{-1}, 1536 cm^{-1}, and 1329 cm^{-1} correspond to C═O stretching (amide I), N—H bending (amide II), and C—N stretching (amide III), respectively (Dong et al., 2018). Moreover, peaks for C—H stretching vibration (~2900 cm^{-1}), C═O stretching vibration (~1745 cm^{-1}), and C—O stretching (~1035 cm^{-1}) were also detected (Zhang et al., 2022). The primary functional groups in the film matrix were

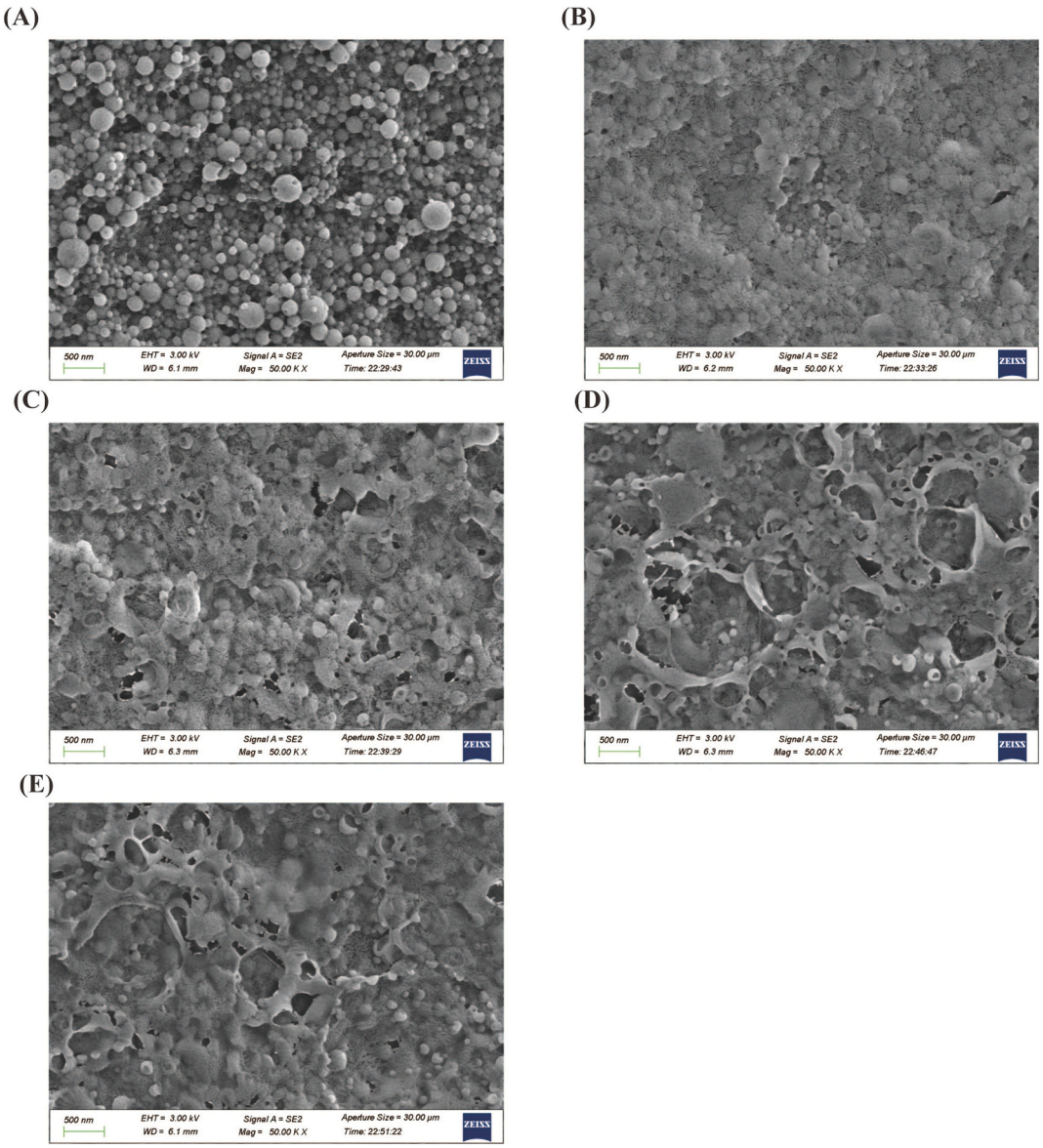

Fig. 2. The SEM images of (A) zein-SC1, (B) zein-SC2, (C) zein-SC5, (D) zein-SC10, (E) zein-SC20.

hydroxyl groups, which can interact with added substances, altering their positions and vibrations in the FTIR spectrum. However, we did not observe any new peaks on addition of ZCNPs, compared to films without nanoparticles, indicating that no new chemical bonds were formed between the ZCNPs and the films. The incorporation of ZCNPs did not alter the film structure. We observed that the addition of ZCNPs shifted the peaks in the amide A region, amide I, and amide II to the right, most likely due to the formation of hydrogen bonds between the film and ZCNPs, which reduces the stretching vibration of free O—H and N—H groups. The hydrogen bond formation has the potential to improve the mechanical properties and thermal stability of the films (Zhang et al., 2022).

3.2.3. XRD

X-ray diffraction (XRD) was employed to analyze the crystal structure of the composite films. Fig. 4B shows that no sharp peaks were detected in any of the films, and the XRD curves of the four sets of films were quite similar. This indicates good compatibility between ZCNPs and the films. The diffraction peak at $2\theta = 9.5$ °corresponds to the relatively regular lattice of chitosan, while a broad peak at $2\theta = 19.6°$ reveals the amorphous structure of the film (Pérez-Córdoba et al., 2017). According to PCSN0, the addition of CS reduces the crystallinity of the original highly crystalline PVA. This may be due to interactions between CS and PVA molecules that disrupt the structure between PVA and CS molecules, making it difficult for PVA molecules to arrange into an ordered crystalline structure, resulting in broader peaks (Yu et al., 2017). There were no new diffraction peaks identified with the addition of ZCNPs, rather the diffraction peaks weakened although not significantly. This indicates that ZCNPs are uniformly mixed in the CS/PVA film and undergo hydrogen bonding and electrostatic interactions, as evidenced in FTIR (Sun et al., 2020).

3.3. Thermal stability of PCSN films

Thermogravimetric analysis (TGA) is used to study the changes in material mass at different temperatures. As the temperature increases, the film begins to decompose, resulting in a loss in mass, the disappearance of intermolecular forces, and the breakage of chemical bonds (El-Sayed, Mahmoud, Fatah, & Hassen, 2011). TGA was performed to evaluate the effect of ZCNPs on the thermal stability of the film. Fig. 4C shows the TG curves of films with different concentrations of ZCNPs. The three main stages of weight loss can be distinguished as the temperature

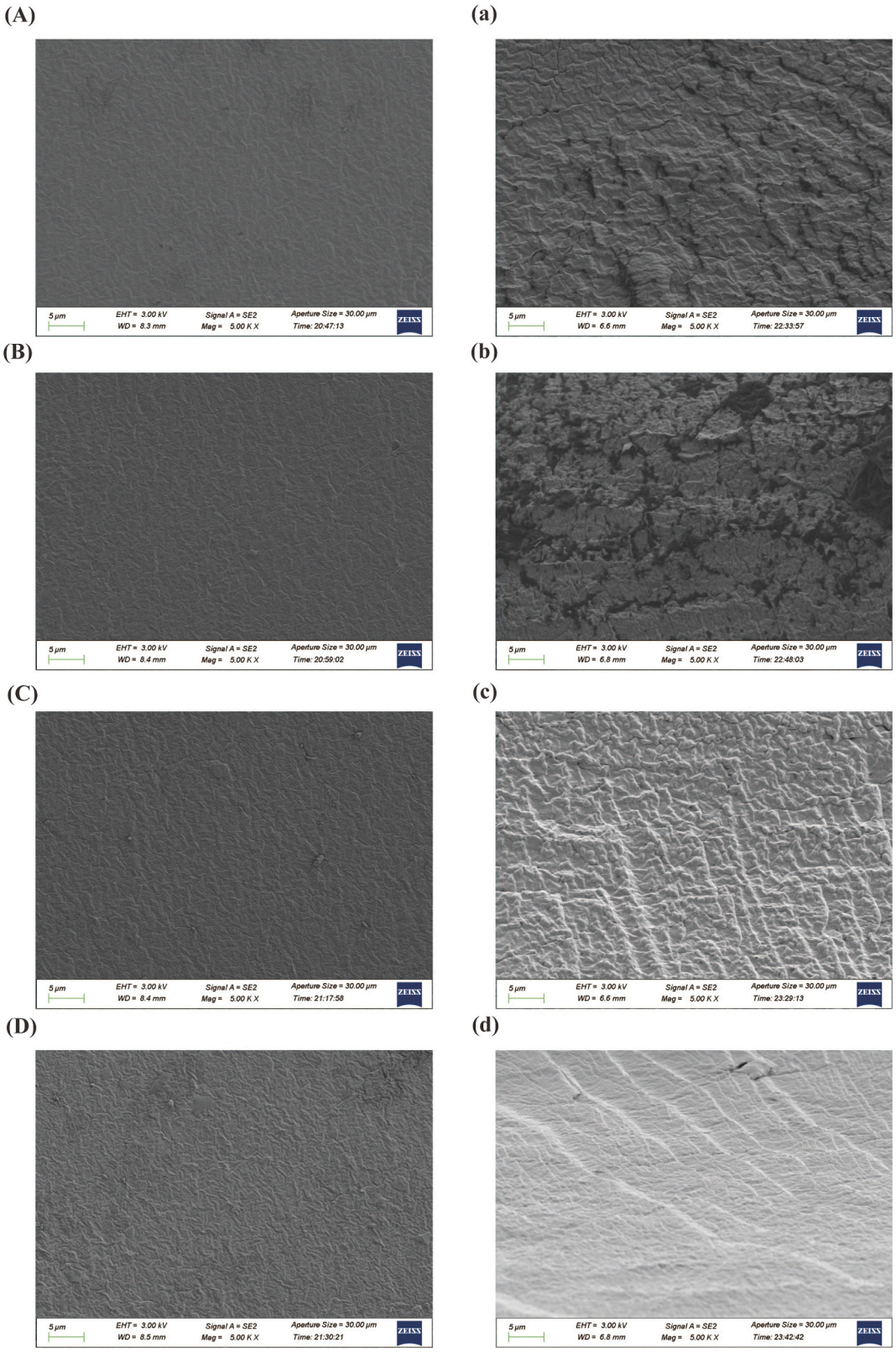

Fig. 3. SEM images of the surface and cross-section of PCSN0 (A) and (a), PCSN5 (B) and (b), PCSN10 (C) and (c), PCSN15 (D) and (d) films.

rises. The first stage, which occurs between 60 °C and 160 °C, is mainly due to the evaporation of bound water in the film, resulting in a slight decrease in weight (Liu, Cai, Jiang, Wu, & Le, 2015). The second stage, which occurs between 170 °C and 260 °C, is characterized by a decrease in mass as a result of glycerol evaporation in the film, denaturation of amino groups in chitosan, and decomposition of zein (Alves Breda, Morgado, Assis, & Duarte, 2017). The third stage occurs between 280 °C to 450 °C, and is primarily involved in the decomposition of PVA/CS and the subsequent decomposition of zein (Wang et al., 2018). In the first stage, no difference was observed in the TGA curves of the various films,

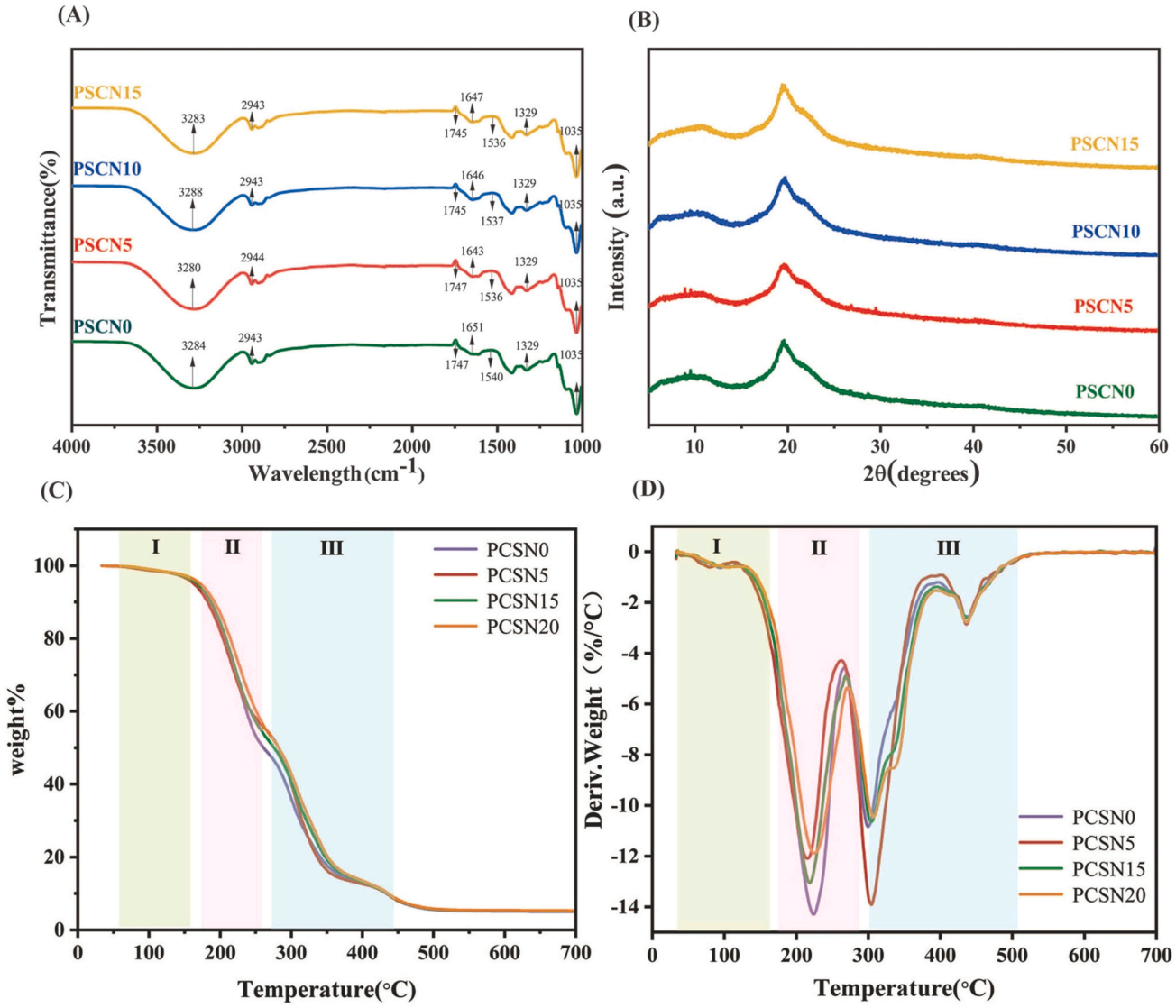

Fig. 4. (A) FTIR, (B) XRD, (C) TGA, (D) DTG for PCSN films.

indicating that the addition of ZCNPs has no effect on water evaporation. The second and third stages show that PCSN0 requires a lower temperature than PCSN5, PCSN10, and PCSN15 under the identical mass loss conditions. This suggests that ZCNPs can enhance the stability of the film, perhaps due to the molecular interactions and hydrogen bonding between nanoparticles and the film. Previous research has shown that uniform distribution of nanoparticles in the film matrix can decrease the mobility of polymer chains and increase thermal stability (Amjadi, Almasi, Ghorbani, & Ramazani, 2020).

Through DTG curves (Fig. 4D), we found that with the addition of nanoparticles, the peak temperature of PCSN0 in the third stage, which was initially 298 °C, shifted to higher temperatures as ZCNPs increased. Specifically, PCSN5, PCSN10, and PCSN15 shifted to 302 °C, 305 °C, and 308 °C, respectively. These findings demonstrate that the addition of ZCNPs enhances the thermal stability of the film.

3.4. Mechanical and physical characteristics of PCSN films

3.4.1. Thickness of PCSN films

Thickness is an important parameter for biodegradable food packaging films since it influences overall mechanical and barrier properties. As shown in Table 1, the thickness of the four films was typically similar, and the addition of ZCNPs had minimal effect on the film thickness. This is consistent with the Zhou, Han, McClements, Cheng, and Chen (2024), where anthocyanin-zein-cinnamaldehyde-carrageenan (AZCC) composite nanoparticles prepared via the anti-solvent co-precipitation method were incorporated into carrageenan films. However, Hu et al. (2023) found that the thickness of gelatin films incorporating allicin-zein composite nanoparticles, prepared using a combination of anti-solvent precipitation and electrostatic deposition, was directly

Table 1
Mechanical and physical properties of PCSN films.

Sample	Thickness (μm)	Tensile strength (MPa)	EAB (%)	WVP ($\times 10^{-6}$ g. m/m^2. s. Pa)
PCSN0	0.32 ± 0.021^a	17.56 ± 0.325^b	181.76 ± 35.31^a	1.28 $\times 10^{-6}$ ± 0.14^a
PCSN5	0.30 ± 0.020^a	12.40 ± 0.915^c	67.52 ± 3.88^b	1.09$\times 10^{-6}$ ± 0.12^{ab}
PCSN10	0.29 ± 0.010^a	24.25 ± 2.745^a	169.10 ± 11.54^a	1.02$\times 10^{-6}$ ± 0.06^b
PCSN15	0.33 ± 0.011^a	14.66 ± 0.910^c	158.07 ± 39.26^a	1.05$\times 10^{-6}$ ± 0.08^b

Data are expressed as mean ± standard deviation. Different letters in the same column indicate the significant differences ($p \leq 0.05$).

proportional to the nanoparticle content. The disparities in findings may be due to the variations in the bioactive components included and the varied film-forming matrices used.

3.4.2. Mechanical properties

Mechanical properties affect the physical protection offered by packaging films during transportation, storage, and usage. Excellent mechanical properties prevent the packaging film from breaking under stress during usage, thus protecting food from contamination and external conditions. Testing the TS and EAB of the films, Table 1 shows that adding 10 % *v*/v of ZCNPs significantly increases the TS of the films ($P < 0.05$). This may be because the ZCNPs are uniformly dispersed in the film matrix, limiting molecular mobility within the matrix. Furthermore, the ZCNPs embedded in the film have the ability to transfer stress from the film to themselves, improving its mechanical properties (Trinh, Chang, & Mekonnen, 2021). Moreover, electrostatic interactions, hydrogen bonding, and the formation of Schiff bases between the ZCNPs and the film elevate the TS of the film. The addition of ZCNPs reduces the EAB ($P < 0.05$), indicating that the inclusion of nanoparticles augments the microstructure of the film, decreases the mobility of the film matrix, and thereby restricts the movement of macromolecules within the film matrix (Zhang, Liu, Sun, Wang, & Li, 2019). However, when the concentration of ZCNPs is increased to 15 %, the mechanical properties of the film decrease. This reduction is due to the formation of aggregates at high ZCNPs concentrations, which leads to changes in the film's microstructure and uneven stress transfer between the particles and the film matrix, thereby compromising the film's compactness. Overall, the incorporation of an adequate amount of ZCNPs significantly increases the mechanical properties of the film, establishing a solid foundation for its application in food packaging.

3.4.3. Moisture content (MC), swelling index (SI) and water solubility (WS)

Fig. 5 shows the moisture content, swelling index, and water solubility of the film. The addition of ZCNPs significantly increased the moisture content of the film as compared to CS/PVA films ($P < 0.05$). The moisture content of the film after adding 15 % *v*/v ZCNPs is 20.44 %. The increase in moisture content of the film may be due to the formation of voids on the film surface following the addition of ZCNPs, resulting in a porous structure that allows more water molecules to penetrate into the film matrix (Evangelho et al., 2019). The swelling index of the film determines its stability. Generally, a higher swelling index indicates lower film stability, making it necessary to add nanoparticle stabilizers, such as zein-tannic acid nanoparticles, to maintain its performance (Li et al., 2023). According to Fig. 5B, the SI of the film decreases with the addition of ZCNPs, highlighting that ZCNPs can enhance the stability of the film. This may be because ZCNPs fill the film, forming a denser matrix.

The water solubility of the film increases as the ZCNPs content increases. Compared to CS/PVA films, adding 10 % *v*/v ZCNPs and 15 % v/v ZCNPs increases the water solubility of the film to 40.82 % and 48.51 %, respectively. Water solubility is determined by the type of polymer in the film and its hydrophilicity. PVA itself has a high hydrophilicity. The addition of nanoparticles leads to an irregular surface structure of the film, which helps increase the contact area between the film and water molecules. This may also contribute to enhancing the film's water solubility. Furthermore, fluctuations in the percentage of glycerol in the total volume of the film-forming solution during the film manufacturing process can affect the water solubility of the film (Mondéjar-López et al., 2023). On the contrary, Lin et al. (2023) found that the water solubility (WS) of gelatin films loaded with eugenol-loaded sodium caseinate and trimethyl chitosan composite nanoparticles (ESTNPs) decreased as the ESTNPs content increased. These findings imply that hydrogen bonds formed between gelatin and ESTNPs, as well as the hydrophobic nature of ESTNPs, restrict the film's water absorption in the environment, reducing its water solubility.

3.4.4. Water vapor permeability (WVP)

Water Vapor Permeability (WVP) testing is an important parameter for assessing the barrier properties of packaging materials. A lower WVP can reduce the moisture permeability from inside and outside the food, minimizing the impact of moisture on the food. The WVP data obtained from measuring the films are shown in Table 1. The WVP of pure PVA/CS film is 1.28×10^{-6} g/m^2. The addition of nanoparticles significantly decreases WVP ($P < 0.05$), measuring 1.09×10^{-6} g/m^2, 1.02×10^{-6} g/m^2, and 1.05×10^{-6} g/m^2, respectively (Table 1). This indicates that the addition of nanoparticles improves the barrier properties of the film against moisture permeation. The decrease in WVP may be attributed to the uniform loading of nanoparticles in the film matrix generates a convoluted path for water molecules to enter, resulting in resistance to their movement (Guo, Ge, Li, Mu, & Li, 2014).

3.4.5. Antioxidative activity of PCSN films

One of the primary causes of food spoilage is oxidation due to contact with oxygen. Using nanocomposite films as food packaging should minimize oxygen permeability, thus protecting the food. We employed DPPH radical scavenging to assess the antioxidant properties of four groups of films. DPPH is a stable free radical that accepts an electron or a hydrogen radical to form a stable diamagnetic molecule (Ksouda et al., 2019). Fig. 6A illustrates that adding 15 % *v*/v ZCNPs increased the radical scavenging rate to 95.4 %. The pure PVA/CS films exhibited lower antioxidant activity, which might linked to the gas barrier properties of CS, which are attributed to the -OH and -NH_2 groups in the multifunctional composite material (Jayakumar, Radoor, Shin, Siengchin, & Kim, 2023). The antioxidant activities of PCSN5 and PCSN10 were 88.4 % and 94.3 %, respectively, suggesting that the addition of ZCNPs enhanced the antioxidant properties of the films. This enhancement is attributed to cinnamaldehyde's radical scavenging capacity as a

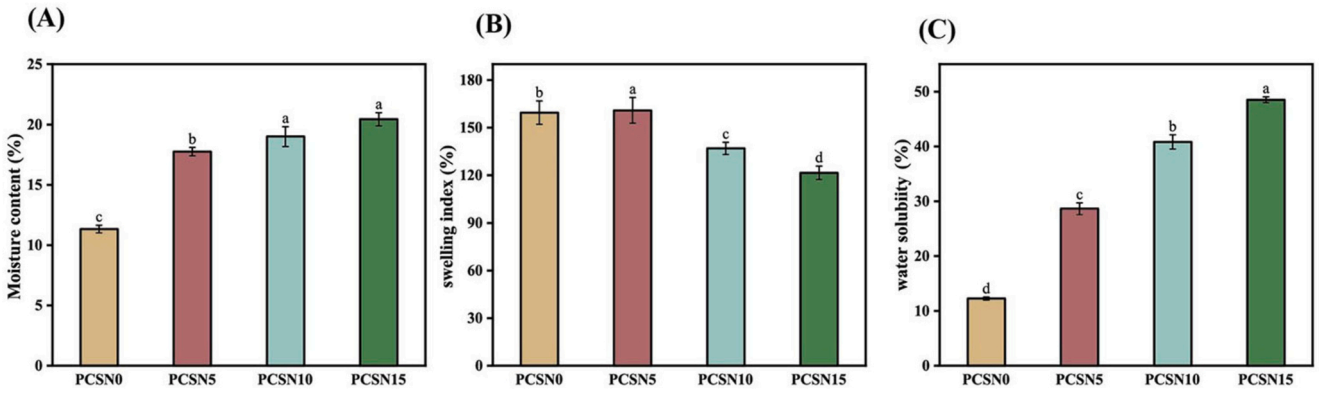

Fig. 5. (A) Moisture Content, (B) Swelling Index, (C) Water Solubility of PCSN films.

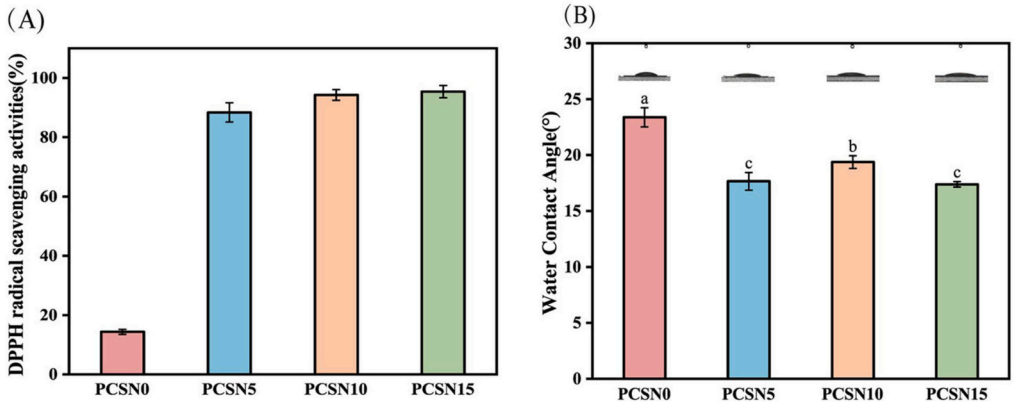

Fig. 6. Antioxidant activity against (A) DPPH radicals, (B) Water Contact Angle of PCSN films.

polyphenol and its hydrophobic nature. Furthermore, the interaction between the aldehyde groups in cinnamaldehyde (CIN) and the amino groups in chitosan (CH) to form Schiff bases improves the antioxidant properties of the films. Wang et al. (2024) validated this conclusion by incorporating zein-loaded cinnamaldehyde (Cin@ZN) nanoparticles into chitosan (CS)/dialdehyde carboxymethyl cellulose (DCMC) matrices.

3.4.6. *Water contact angle (WCA)*

Water contact angle is widely used to assess the wettability of

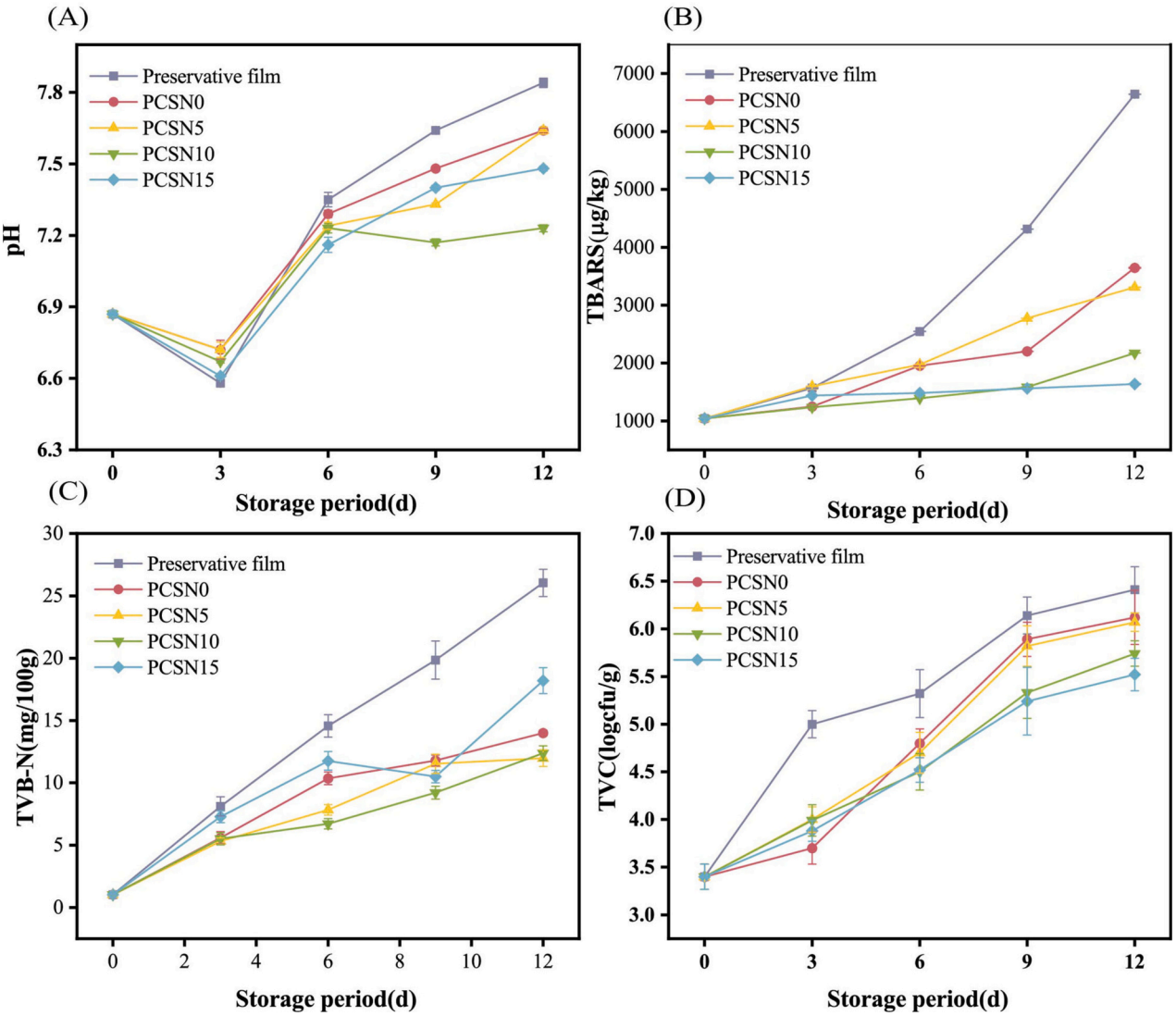

Fig. 7. Changes in Total pH. (A) Thiobarbituric Acid Reactive Substances, (B) Volatile Basic Nitrogen, (C) Total viable counts, (D) of pomfret fish stored at 4 °C for 12 days.

material surfaces. Studies show that a water contact angle greater than 90° is hydrophobic, while a water contact angle less than 90° is hydrophilic (Pizarro et al., 2020). Fig. 6B demonstrates the water contact angles of PCSN0, PCSN5, PCSN10, and PCSN15 as 23.4°, 17.7°, 19.3°, and 17.4°, respectively. The water contact angle of the CS/PVA film without added nanoparticles is 23.4°. This may be ascribed to the increased hydrophilicity of CS/PVA generated by the addition of PVA as well as the ability of glycerol to bind with water. We discovered that the water contact angle decreased as the nanoparticles increased. The addition of nanoparticles causes the film surface to become rough, with small particle protrusions and irregular wrinkles. This is also a key factor contributing to the decrease in the WCA value. When added to the CS/PVA film, they reduce the water contact angle (Chen et al., 2022). In addition, hydrophilic films are readily biodegraded by microorganisms, allowing for degradation in natural habitats and reducing pollution for environmental protection (Liu, Li, Li, et al., 2022).

3.5. Preservation of pomfret fish with PCSN films

3.5.1. pH

pH is an important indicator of meat freshness. As shown in Fig. 7A, when silver pomfret is subjected to different treatments and stored at 4 °C, the pH initially drops and subsequently rises. This tendency occurs because, during the early stages of storage, the glycogen in silver pomfret breaks down into lactic acid and other acidic substances that cannot be metabolized, leading to a decrease in pH (Zhao et al., 2021). In the later stages of storage, the spoilage of silver pomfret results in the production of spoilage bacteria and endogenous enzymes, which break down proteins into ammonia, amines, and other alkaline substances, resulting in an elevation in pH (Wang, Hu, Gao, Ye, & Wang, 2017). The pH increased rapidly in PCSN0 and plastic wrap than in films with added ZCNPs. By the 12th day, the pH of silver pomfret wrapped in plastic reached 7.84, compared to 7.23 for PCSN15 on the same day, indicating that ZCNPs-loaded films effectively inhibit protein degradation and spoilage, thereby slowing the decline in quality of silver pomfret.

3.5.2. TBARS

Lipid oxidation impairs the quality of silver pomfret. Fig. 7B shows that the degree of lipid oxidation in silver pomfret treated with different films varies. The TBARS value of plastic-wrapped silver pomfret increased from 0.104 mg MDA/kg to 0.664 mg MDA/kg by the 12th day. On the 12th day, silver pomfret treated with PCSN10 and PCSN15 had TBARS levels of 0.217 mg MDA/kg and 0.163 mg MDA/kg, respectively, which decreased by 67.3 % to 75.4 % compared to the control group. This may be attributed to the excellent oxygen barrier properties of the film, which prevent oxygen from coming into contact with the silver pomfret, thereby reducing lipid oxidation. However, chitosan contains free amino groups that can scavenge free radicals and produce stable fluorescent compounds with volatile aldehydes such as malondialdehyde, lowering the rise in TBARS values (Hosseini et al., 2021). Moreover, cinnamaldehyde, a primary component of plant essential oils, contains phenolic and aldehyde components that efficiently prevent lipid oxidation. When loaded onto nanoparticles, it achieves a controlled release effect, prolonging the duration of antioxidant protection (Cai et al., 2020).

3.5.3. TVB-N

Total volatile basic nitrogen (TVB-N) is the product of protein degradation in meat during storage caused by microorganisms and endogenous enzymes. It can serve as an indicator of meat freshness (Bekhit, Holman, Giteru, & Hopkins, 2021). Fig.7C depicts the variations in TVB-N content of silver pomfret stored for 12 days under different film packaging. The control group showed a rapid increase from 1.03 mg/100 g on the first day to 26.04 mg/100 g on the 12th day. PCSN10 and PCSN5 reduced protein degradation from 52.5 % to 30.1 % when compared to the control group. This signifies that PCSN film effectively suppress microbial-induced protein degradation. This may be due to the addition of ZCNPs to the film resulting in a uniform and dense matrix, preventing the permeation of water vapor and oxygen. Furthermore, cinnamaldehyde, a natural active ingredient, has excellent antibacterial properties when stably released in the film, limiting the rise in TVB-N levels. This is consistent with the findings of Wang et al. (2022), who successfully delayed the increase in TVB-N in golden pomfret fillets by coating them with chitosan-grapefruit seed oil and employing modified atmosphere packaging. Overall, these data demonstrate that PCSN films effectively inhibit lipid changes as well as amine and ammonia formation in silver pomfret.

3.5.4. TVC

Bacterial growth and reproduction are the primary causes of rapid deterioration in the silver pomfret. As shown in Fig.7D, the TVC (Total Viable Count) of silver pomfret wrapped in different film compositions showed an increasing trend throughout a 12-day storage process at 4 °C. At the beginning of storage, the TVC of silver pomfret was 3.4 log CFU/g. As time progressed until the 12th day, the TVC of silver pomfret wrapped in preservation film ascended to 7.41 log CFU/g, whereas that wrapped in PCSN15 was 5.92 log CFU/g, showing a significant decrease of 1.49 log CFU/g compared to the preservation film. This may be because the PCSN film contains active ingredients of cinnamaldehyde, which can reduce the bacterial reproduction rate by synthesizing bacterial cell walls and maintaining the integrity of cell membranes (Shreaz et al., 2016). Moreover, cinnamaldehyde encapsulated in nanoparticles releases gradually over 12 days, extending the storage time of the silver pomfret. Therefore, the addition of cinnamaldehyde nanoparticles to the film inhibits bacterial growth, preventing the quality deterioration of the silver pomfret.

4. Conclusion

In this study, cinnamaldehyde-loaded zein nanoparticles coated with sodium alginate were successfully prepared via an anti-solvent co-precipitation method, resulting in an average particle size of 196 nm, a zeta potential of −35 mV, and a PDI of less than 0.3. Experimental results confirmed that sodium alginate coating could stably enhance particle size, zeta potential, and PDI properties of the nanoparticles. ZCNPs were added to a CS/PVA mixed film-forming solution to prepare the films. The results indicated that the incorporation of ZCNPs enhanced the mechanical, barrier, and antioxidant properties of the films. To be specific, compared to PCSN0, TS of PCSN10 increased by 23 %, while the EAB decreased by 8.5 %, thus enhancing the protective capacity of the packaging for food products. Compared to PCSN0, the WVP of PCSN15 decreased by 21.9 %, reducing the impact of moisture on food. FTIR and XRD analyses revealed the molecular interactions between ZCNP and the films. Additionally, the radical scavenging capacity of the films with 15 % ZCNPs reached over 90 %, effectively reducing lipid oxidation. When applied to the preservation of silver pomfret, the TVC decreased from 6.38 log (CFU/g) to 5.41 log (CFU/g), TVB-N decreased by 25.5 %, and TBARS decreased by 69 %, significantly slowing the spoilage and deterioration during storage. This study demonstrates that chitosan/polyvinyl alcohol films incorporated with cinnamaldehyde nanoparticles are bioactive food packaging films with favorable physicochemical properties, holding great potential for seafood packaging.

CRediT authorship contribution statement

Zhan Zhang: Writing – original draft, Software, Methodology, Investigation, Data curation, Conceptualization. **Xiaojun Zhang:** Writing – review & editing, Investigation, Formal analysis, Conceptualization. **Bing Lin:** Methodology, Investigation, Data curation. **Yaqian Zhong:** Writing – review & editing, Supervision. **Wenxiu Zhang:** Investigation. **Shangrong Zhong:** Investigation. **Xiaxia Chen:** Project administration, Funding acquisition, Conceptualization.

Declaration of competing interest

The authors declare that they have no known competing financial interests or personal relationships that could have appeared to influence the work reported in this paper.

Data availability

The data that has been used is confidential.

References

Al-Maqtari, Q., Al-Gheethi, E. I. A., Ghaleb, A., Mahdi, A., Al-Ansi, W., Noman, A., Yao, W., et al. (2022). Fabrication and characterization of chitosan/gelatin films loaded with microcapsules of Pulicaria jaubertii extract. *Food Hydrocolloids, 129*, Article 107624. https://doi.org/10.1016/j.foodhyd.2022.107624

Alves Breda, C., Morgado, D., Assis, O., & Duarte, M. (2017). Processing and characterization of chitosan films with incorporation of ethanolic extract from "Pequi" peels. *Macromolecular Research, 1-8*. https://doi.org/10.1007/s13233-017-5143-4

Amjadi, S., Almasi, H., Ghorbani, M., & Ramazani, S. (2020). Preparation and characterization of TiO2NPs and betanin loaded zein/sodium alginate nanofibers. *Food Packaging and Shelf Life, 24*, Article 100504. https://doi.org/10.1016/j.fpsl.2020.100504

Ban, Z. J., Niu, C. Y., Li, L., Gao, Y. Z., Liu, L. L., Lu, J. C., Chen, C. K., et al. (2024). Exogenous brassinolides and calcium chloride synergically maintain quality attributes of jujube fruit (Ziziphus jujuba Mill.). *Postharvest Biology and Technology, 216*. https://doi.org/10.1016/j.postharvbio.2024.113039

Bekhit, A., Holman, B., Giteru, S., & Hopkins, D. (2021). Total volatile basic nitrogen (TVB-N) and its role in meat spoilage: A review. *Trends in Food Science & Technology, 109*, 280–302. https://doi.org/10.1016/j.tifs.2021.01.006

Cai, C., Ma, R., Duan, M., Deng, Y., Liu, T., & Lu, D. (2020). Effect of starch film containing thyme essential oil microcapsules on physicochemical activity of mango. *LWT, 131*, Article 109700. https://doi.org/10.1016/j.lwt.2020.109700

Chang, C., Wang, T., Hu, Q., & Luo, Y. (2017). Zein/caseinate/pectin complex nanoparticles: Formation and characterization. *International Journal of Biological Macromolecules, 104*. https://doi.org/10.1016/j.ijbiomac.2017.05.178

Chen, H., Hu, X., Chen, E., Wu, S., McClements, D., Liu, S., et al.Li, Y. (2016). Preparation, characterization, and properties of chitosan films with cinnamaldehyde nanoemulsions. *Food Hydrocolloids, 61*. https://doi.org/10.1016/j.foodhyd.2016.06.034

Chen, S., Ma, Y., Dai, L., Liao, W., Zhang, L., Liu, J., & Gao, Y. (2021). Fabrication, characterization, stability and re-dispersibility of curcumin-loaded gliadin-rhamnolipid composite nanoparticles using pH-driven method. *Food Hydrocolloids, 118*, Article 106758. https://doi.org/10.1016/j.foodhyd.2021.106758

Chen, Y., Liu, C., Yang, Z., Sun, Y., Chen, X., & Liu, L. (2022). Fabrication of zein-based hydrophilic nanoparticles for efficient gene delivery by layer-by-layer assembly. *International Journal of Biological Macromolecules, 217*. https://doi.org/10.1016/j.ijbiomac.2022.07.042

Chen, Y., Liu, Y., Dong, Q., Xu, C., Deng, S., Kang, Y., et al.Li, L. (2023). Application of functionalized chitosan in food: A review. *International Journal of Biological Macromolecules, 235*, Article 123716. https://doi.org/10.1016/j.ijbiomac.2023.123716

Davidov-Pardo, G., Joye, I., & McClements, D. (2015). Encapsulation of resveratrol in biopolymer particles produced using liquid antisolvent precipitation. Part 1: Preparation and characterization. *Food Hydrocolloids, 45*. https://doi.org/10.1016/j.foodhyd.2014.11.023

Dong, S., Guo, P., Chen, Y., Chen, G.-Y., Ji, H., Ran, Y., et al.Chen, Y. (2018). Surface modification via atmospheric cold plasma (ACP): Improved functional properties and characterization of zein film. *Industrial Crops and Products, 115*, 124–133. https://doi.org/10.1016/j.indcrop.2018.01.080

Doyle, A., & Stephens, J. (2019). A review of cinnamaldehyde and its derivatives as antibacterial agents. *Fitoterapia, 139*, Article 104405. https://doi.org/10.1016/j.fitote.2019.104405

El-Sayed, S., Mahmoud, K., Fatah, A., & Hassen, A. (2011). DSC, TGA and dielectric properties of carboxymethyl cellulose/polyvinyl alcohol blends. *Physica B-condensed Matter - PHYSICA B, 406*, 4068–4076. https://doi.org/10.1016/j.physb.2011.07.050

Evangelho, J., Dannenberg, G., Biduski, B., Halal, S., Kringel, D., Gularte, M., et al. Zavareze, E. (2019). Antibacterial activity, optical, mechanical, and barrier properties of corn starch films containing orange essential oil. *Carbohydrate Polymers, 222*, Article 114981. https://doi.org/10.1016/j.carbpol.2019.114981

Fan, W., Yan, W., Xu, Z., & Ni, H. (2012). Formation mechanism of monodisperse, low molecular weight chitosan nanoparticles by ionic gelation technique. *Colloids and surfaces. B, Biointerfaces, 90*, 21–27. https://doi.org/10.1016/j.colsurfb.2011.09.042

Guo, J., Ge, L., Li, X., Mu, C., & Li, D. (2014). Periodate oxidation of xanthan gum and its crosslinking effects on gelatin-based edible films. *Food Hydrocolloids, 39*, 243–250. https://doi.org/10.1016/j.foodhyd.2014.01.026

Guo, Q. W., Cui, B., Yuan, C., Guo, L., Li, Z., Chai, Q. Q., Zhao, M., et al. (2024). Fabrication of dry S/O/W microcapsule and its probiotic protection against different stresses. *Journal of the Science of Food and Agriculture, 104*(5), 2842–2850. https://doi.org/10.1002/jsfa.13175

Haghighi, H., Gullo, M., La China, S., Siesler, H., Licciardello, F., & Pulvirenti, A. (2020). Characterization of bio-nanocomposite films based on gelatin/polyvinyl alcohol blend reinforced with bacterial cellulose nanowhiskers for food packaging applications. *Food Hydrocolloids, 113*. https://doi.org/10.1016/j.foodhyd.2020.106454

Hosseini, S. F., Ghaderi, J., & Gómez-Guillén, M. (2021). Tailoring physico-mechanical and antimicrobial/antioxidant properties of biopolymeric films by cinnamaldehyde-loaded chitosan nanoparticles and their application in packaging of fresh rainbow trout fillets. *Food Hydrocolloids, 124*, Article 107249. https://doi.org/10.1016/j.foodhyd.2021.107249

Hosseini, S. F., & Gómez-Guillén, M. (2018). A state-of-the-art review on the elaboration of fish gelatin as bioactive packaging: Special emphasis on nanotechnology-based approaches. *Trends in Food Science & Technology, 79*. https://doi.org/10.1016/j.tifs.2018.07.022

Hu, K., & McClements, D. (2015). Fabrication of biopolymer nanoparticles by antisolvent precipitation and electrostatic deposition: Zein-alginate core/shell nanoparticles. *Food Hydrocolloids, 44*, 101–108. https://doi.org/10.1016/j.foodhyd.2014.09.015

Hu, L., Zhao, P., Wei, Y., Guo, X., Deng, X., & Zhang, J. (2023). Properties of Allicin–Zein Composite Nanoparticle Gelatin Film and Their Effects on the Quality of Cold, Fresh Beef during Storage. *Foods, 12*, 3713. https://doi.org/10.3390/foods12193713

Hua, L., Deng, J., Wang, Z., Wang, Y., Chen, B., Ma, Y., et al.Xu, B. (2021). Improving the functionality of chitosan-based packaging films by crosslinking with nanoencapsulated clove essential oil. *International Journal of Biological Macromolecules, 192*. https://doi.org/10.1016/j.ijbiomac.2021.09.197

Huang, X., Ge, X., Zhou, L., & Wang, Y. (2022). Eugenol embedded zein and poly(lactic acid) film as active food packaging: Formation, characterization, and antimicrobial effects. *Food Chemistry, 384*, Article 132482. https://doi.org/10.1016/j.foodchem.2022.132482

Jayakumar, A., Radoor, S., Shin, G., Siengchin, S., & Kim, J. T. (2023). Active and intelligent packaging films based on PVA/Chitosan/Zinc oxide nanoparticles/Sweet purple potato extract as pH sensing and antibacterial wraps. *Food Bioscience, 56*, Article 103432. https://doi.org/10.1016/j.fbio.2023.103432

Ksouda, G., Sellimi, S., Merlier, F., Falcimaigne-cordin, A., Thomasset, B., & Mohamed, H. (2019). Composition, antibacterial and antioxidant activities of Pimpinella saxifraga essential oil and application to cheese preservation as coating additive. *Food Chemistry, 288*. https://doi.org/10.1016/j.foodchem.2019.02.103

Li, S., Liu, X., Zhang, X., Wang, F., Zhou, J., & Zhang, H. (2023). Preparation and characterization of zein-tannic acid nanoparticles/chitosan composite films and application in the preservation of sugar oranges. *Food Chemistry, 437*, Article 137673. https://doi.org/10.1016/j.foodchem.2023.137673

Li, Y., Yang, J., Sun, L., Liu, B., Li, H., & Peng, L. (2023). Crosslinked fish scale gelatin/alginate dialdehyde functional films incorporated with carbon dots derived from pomelo peel waste for active food packaging. *International Journal of Biological Macromolecules, 253*, Article 127290. https://doi.org/10.1016/j.ijbiomac.2023.127290

Lim, H.-P., Ho, K.-W., Singh, C., Ooi, C.-W., Tey, B. T., & Chan, E. (2020). Pickering emulsion hydrogel as a promising food delivery system: Synergistic effects of chitosan Pickering emulsifier and alginate matrix on hydrogel stability and emulsion delivery. *Food Hydrocolloids, 103*, Article 105659. https://doi.org/10.1016/j.foodhyd.2020.105659

Lin, L., Mei, C., Shi, C., Li, C.-Z., Abdel-Samie, M., & Cui, H. (2023). Preparation and characterization of gelatin active packaging film loaded with eugenol nanoparticles and its application in chicken preservation. *Food Bioscience, 53*, Article 102778. https://doi.org/10.1016/j.fbio.2023.102778

Lin, W., Zhang, Y., Huang, J., & Li, Z. (2023). pH-responsive double-layer film based on chitosan/curcumin-β-cyclodextrin complex/cinnamaldehyde and zein/alizarin for pork freshness monitoring and maintaining. *Food Research International, 173*, Article 113460. https://doi.org/10.1016/j.foodres.2023.113460

Liu, F., Zhang, X.-W., Xing-Long, X., Duan, Q., Bai, H., Cao, Y., et al.Yu, L. (2023). Improved hydrophobicity, antibacterial and mechanical properties of polyvinyl alcohol/quaternary chitosan composite films for antibacterial packaging. *Carbohydrate Polymers, 312*, Article 120755. https://doi.org/10.1016/j.carbpol.2023.120755

Liu, Q., Jing, Y., Han, C., Zhang, H., & Tian, Y. (2019). Encapsulation of curcumin in zein/ caseinate/sodium alginate nanoparticles with improved physicochemical and controlled release properties. *Food Hydrocolloids, 93*. https://doi.org/10.1016/j.foodhyd.2019.02.003

Liu, Q., Li, B., Li, Y., Yang, X., Wang, S., Qiao, C., & Wang, N. (2022). Cross-linked films based on N-hydrophobic-O-hydrophilic chitosan derivatives: Preparation, properties and application in banana storage. *Food Hydrocolloids, 135*, Article 108113. https://doi.org/10.1016/j.foodhyd.2022.108113

Liu, Q., Li, Y., Zhou, Y., Jiang, L., Lyu, Q., Liu, G., et al.Chen, L. (2022). Zein-whey protein isolate-carboxymethyl cellulose complex as carrier of apigenin via pH-driven method: Fabrication, characterization, stability, and in vitro release property. *Food Chemistry, 387*, Article 132926. https://doi.org/10.1016/j.foodchem.2022.132926

Liu, Y., Cai, Y., Jiang, X., Wu, J., & Le, X.-Y. (2015). Molecular interactions, characterization and antimicrobial activity of curcumin-chitosan blend films. *Food Hydrocolloids, 52*. https://doi.org/10.1016/j.foodhyd.2015.08.005

Ludwicka, K., Kaczmarek, M., & Białkowska, A. (2020). Bacterial Nanocellulose—A Biobased Polymer for Active and Intelligent Food Packaging Applications: Recent Advances and Developments. *Polymers, 12*, 2209. https://doi.org/10.3390/polym12102209

Mondéjar-López, M., Castillo-López, R., Lopez-Jimenez, A. J., Gómez-Gómez, L., Ahrazem, O., & Niza, E. (2023). Polysaccharide film containing cinnamaldehyde-chitosan nanoparticles, a new eco-packaging material effective in meat preservation.

Food Chemistry, 437, Article 137710. https://doi.org/10.1016/j.foodchem.2023.137710

Narasgoudr, S., Hegde, V., Vanjeri, V., Chougale, R., & Masti, S. (2020). Ethyl Vanillin Incorporated Chitosan/Poly(vinyl alcohol) Active Films For Food Packaging Applications. *Carbohydrate Polymers, 236*, Article 116049. https://doi.org/10.1016/j.carbpol.2020.116049

Panda, P., Sadeghi, K., & Seo, J. (2022). Recent advances in poly (vinyl alcohol)/natural polymer based films for food packaging applications: A review. *Food Packaging and Shelf Life, 33*, Article 100904. https://doi.org/10.1016/j.fpsl.2022.100904

Pérez-Córdoba, L., Norton, I., Batchelor, H., Gkatzionis, K., Spyropoulos, F., & Sobral, P. (2017). Physico-chemical, antimicrobial and antioxidant properties of gelatin-chitosan based films loaded with nanoemulsions encapsulating active compounds. *Food Hydrocolloids, 79*. https://doi.org/10.1016/j.foodhyd.2017.12.012

Pizarro, G., Marambio, O., Jeria-Orell, M., Sánchez, J., Oyarzún, D., Martín Trasancos, R., & Novio, F. (2020). Morphological, optical and wettability characterization of honeycomb patterned films based on self-assembling copolymer under thermal annealing. *Chemical Physics, 533*, Article 110715. https://doi.org/10.1016/j.chemphys.2020.110715

Roy, V., Abdur, M., Ho, R., Duraiarasan, T., Jin-Seok, S. P., & Chun, B.-S. (2022). Fabrication of zein and κ-carrageenan colloidal particles for encapsulation of quercetin: In-vitro digestibility and bio-potential activities. *Journal of Industrial and Engineering Chemistry, 111*. https://doi.org/10.1016/j.jiec.2022.04.007

Shreaz, S., Wani, W., Behbehani, J., Raja, V., Irshad, M., Karched, M., et al.Ting Hun, L. (2016). Cinnamaldehyde and its derivatives, a novel class of antifungal agents. *Fitoterapia, 112*. https://doi.org/10.1016/j.fitote.2016.05.016

Sun, J., Jiang, H., Wu, H., Tong, C., Pang, J., & Wu, C. (2020). Multifunctional bionanocomposite films based on konjac glucomannan/chitosan with nano-ZnO and mulberry anthocyanin extract for active food packaging. *Food Hydrocolloids, 107*, Article 105942. https://doi.org/10.1016/j.foodhyd.2020.105942

Tan, X., Sun, A., Cui, F., Li, Q., Wang, D., Li, X., & Li, J. (2024). The physicochemical properties of Cassava Starch/Carboxymethyl cellulose sodium edible film incorporated of Bacillus and its application in salmon fillet packaging. *Food Chem X, 23*, Article 101537. https://doi.org/10.1016/j.fochx.2024.101537

Trinh, B.-M., Chang, C., & Mekonnen, T. (2021). Facile fabrication of thermoplastic starch/poly (lactic acid) multilayer films with superior gas and moisture barrier properties. *Polymer, 223*, Article 123679. https://doi.org/10.1016/j.polymer.2021.123679

Wang, J., Chen, C., & Xie, J. (2022). Loading oregano essential oil into microporous starch to develop starch/polyvinyl alcohol slow-release film towards sustainable active packaging for sea bass (Lateolabrax japonicus). *Industrial Crops and Products, 188*, Article 115679. https://doi.org/10.1016/j.indcrop.2022.115679

Wang, K., Li, W., Wu, L., Li, Y., & Li, H. (2024). Preparation and characterization of chitosan/dialdehyde carboxymethyl cellulose composite film loaded with cinnamaldehyde@zein nanoparticles for active food packaging. *International Journal of Biological Macromolecules, 261*, Article 129586. https://doi.org/10.1016/j.ijbiomac.2024.129586

Wang, S., Liu, Z., Zhao, M.-T., Gao, C., Wang, J., Li, C., et al.Zhou, D. (2022). Chitosan-wampee seed essential oil composite film combined with cold plasma for refrigerated storage with modified atmosphere packaging: A promising technology for quality preservation of golden pompano fillets. *International Journal of Biological Macromolecules, 224*. https://doi.org/10.1016/j.ijbiomac.2022.10.212

Wang, X., Yong, H., Gao, L., Li, L., Jin, M., & Liu, J. (2018). Preparation and characterization of antioxidant and pH-sensitive films based on chitosan and black soybean seed coat extract. *Food Hydrocolloids, 89*. https://doi.org/10.1016/j.foodhyd.2018.10.019

Wang, Y., Zhang, R., Qin, W., Dai, J., Zhang, Q., Lee, K., & Liu, Y. (2019). Physicochemical properties of gelatin films containing tea polyphenol-loaded chitosan nanoparticles generated by electrospray. *Materials & Design, 185*, Article 108277. https://doi.org/10.1016/j.matdes.2019.108277

Wang, Z., Hu, S., Gao, Y., Ye, C., & Wang, H. (2017). Effect of collagen-lysozyme coating on fresh-salmon fillets preservation. *LWT - Food Science and Technology, 75*. https://doi.org/10.1016/j.lwt.2016.08.032

Wrońska, N., Katir, N., Milowska, K., Hammi, N., Nowak-Lange, M., Kędzierska, M., et al. Lisowska, K. (2021). Antimicrobial Effect of Chitosan Films on Food Spoilage Bacteria. *International Journal of Molecular Sciences, 22*, 5839. https://doi.org/10.3390/ijms22115839

Wu, C., Hu, Y., Chen, S., Chen, J., Liu, D., & Ye, X. (2016). Formation mechanism of nano-scale antibiotic and its preservation performance for silvery pomfret. *Food Control, 69*. https://doi.org/10.1016/j.foodcont.2016.05.020

Yang, X. H., Wang, J. R., Xia, X. Z., Zhang, Z. Q., He, J., Nong, B. X., Deng, G. F., et al. (2021). OsTTG1, a WD40 repeat gene, regulates anthocyanin biosynthesis in rice. *Plant Journal, 107*(1), 198–214. https://doi.org/10.1111/tpj.15285

Yao, K., Chen, W., Song, F., McClements, D., & Hu, K. (2017). Tailoring zein nanoparticle functionality using biopolymer coatings: Impact on curcumin bioaccessibility and antioxidant capacity under simulated gastrointestinal conditions. *Food Hydrocolloids, 79*. https://doi.org/10.1016/j.foodhyd.2017.12.029

Yavari Maroufi, L., Ghorbani, M., Tabibiazar, M., Mohammdi, M., & Pezeshki, A. (2021). Advanced properties of gelatin film by incorporating modified kappa-carrageenan and zein nanoparticles for active food packaging. *International Journal of Biological Macromolecules, 183*. https://doi.org/10.1016/j.ijbiomac.2021.04.163

Ye, G., Wu, T., Li, Z., Teng, M., Ma, L., Qin, M., et al.Fu, Q. (2023). Preparation and characterization of novel composite nanoparticles using zein and hyaluronic acid for efficient delivery of naringenin. *Food Chemistry, 417*, Article 135890. https://doi.org/10.1016/j.foodchem.2023.135890

Yu, Z., Li, B., Chu, J., & Zhang, P. (2017). Silica in situ enhanced PVA/chitosan biodegradable films for food packages. *Carbohydrate Polymers, 184*. https://doi.org/10.1016/j.carbpol.2017.12.043

Zhang, A., Xiankang, F., Zeng, X., Xu, J., Zhou, C., Xia, Q., et al.Pan, D. (2023). Enhancing physicochemical, antimicrobial, and release properties of fish skin gelatin films using dual-layer nanoparticles loaded with tea polyphenols/kojic acid for air-dried chicken preservation. *Food Hydrocolloids, 149*, Article 109580. https://doi.org/10.1016/j.foodhyd.2023.109580

Zhang, H. Y., Zuo, X. Y., Sun, B. Y., Wei, B. Q., Fu, J. J., & Xiao, X. Q. (2023). Fuzzy-PID-Based Atmosphere Packaging Gas Distribution System for Fresh Food. *Applied Sciences-Basel, 13*(4). https://doi.org/10.3390/app13042674

Zhang, L., Chen, D., Yu, D., Regenstein, J., Jiang, Q., Dong, J., et al.Xia, W. (2022). Modulating physicochemical, antimicrobial and release properties of chitosan/zein bilayer films with curcumin/nisin-loaded pectin nanoparticles. *Food Hydrocolloids, 133*, Article 107955. https://doi.org/10.1016/j.foodhyd.2022.107955

Zhang, L., Li, K., Yu, D., Regenstein, J., Dong, J., Chen, W., & Xia, W. (2022). Chitosan/zein bilayer films with one-way water barrier characteristic: Physical, structural and thermal properties. *International Journal of Biological Macromolecules, 200*. https://doi.org/10.1016/j.ijbiomac.2021.12.199

Zhang, L., Liu, Z., Sun, Y., Wang, X., & Li, L. (2019). Effect of α-tocopherol antioxidant on rheological and physicochemical properties of chitosan/zein edible films. *LWT, 118*, Article 108799. https://doi.org/10.1016/j.lwt.2019.108799

Zhao, F., Zhuang, P., Song, C., Shi, Z.-H., & Zhang, L.-Z. (2010). Amino acid and fatty acid compositions and nutritional quality of muscle in the pomfret, Pampus punctatissimus. *Food Chemistry - FOOD CHEM, 118*, 224–227. https://doi.org/10.1016/j.foodchem.2009.04.110

Zhao, R., Guan, W., Zheng, P., Tian, F., Zhang, Z., Sun, Z., & Cai, L. (2021). Development of edible composite film based on chitosan nanoparticles and their application in packaging of fresh red sea bream fillets. *Food Control, 132*, Article 108545. https://doi.org/10.1016/j.foodcont.2021.108545

Zhou, M., Han, Y., McClements, D., Cheng, C., & Chen, S. (2024). Co-encapsulation of anthocyanin and cinnamaldehyde in nanoparticle-filled carrageenan films: Fabrication, characterization, and active packaging applications. *Food Hydrocolloids, 149*, Article 109609. https://doi.org/10.1016/j.foodhyd.2023.109609

Zou, Y., Sun, Y., Shi, W., Wan, B., & Zhang, H. (2022). Dual-functional shikonin-loaded quaternized chitosan/polycaprolactone nanofibrous film with pH-sensing for active and intelligent food packaging. *Food Chemistry, 399*, Article 133962. https://doi.org/10.1016/j.foodchem.2022.133962